In Silico Pharmacology (2024) 12:56
https://doi.org/10.1007/s40203-024-00223-2

ORIGINAL RESEARCH

Exploring gene network and protein interaction analysis of neurotrophin signaling pathway in ameloblastoma

Sidhra Syed Zameer Ahmed[1] · Manimaran Vetrivel[1] · Syed Zameer Ahmed Khader[1] · Yoithapprabhunath Thuckanaickenpalayam Ragunathan[2] · SriChinthu Kenniyan Kumar[3] · Puniethaa Prabhu[1] · Dharani Lakshmi Devi Rajaram[1]

Received: 13 February 2024 / Accepted: 18 May 2024
© The Author(s), under exclusive licence to Springer-Verlag GmbH Germany, part of Springer Nature 2024

Abstract

Ameloblastoma is a non-cancerous but aggressive oral tumor emerging from odontogenic epithelial tissue involved during odontogenesis. Since there is lack in unravelling the complete molecular pathogenesis of ameloblastoma, chemotherapy is less attempted and a lot of disagreement over the optimal treatment option. Hence, till date, wide surgical resection is considered to be the reliable treatment for ameloblastoma. The Neurotrophin Signaling pathway plays an important role in neuron signaling and it is closely related with the MAPK pathway, which on the other hand regulated cell differentiation, apoptosis, proliferation, plasticity and survival. Protein- Protein Interaction analysis was analysed with STRING tool using WNL value, identified that CTNNB1, HRAS, NGFR, NGFR, and SORT1 having high interacting with BDNF, NT4, p75NTR, NGF, and NT3. The results of ontology analysis revealed that Neurotrophin signaling pathway is associated with Cell surface receptor signaling pathway, regulation of cell differentiation, regulation of development process, EGFR tyrosine kinase inhibitor resistance, MAPK signaling pathway, PI3K-Akt signaling pathway and Ras signaling pathway leading to pathogenesis involving genes. Further, clustering coefficient values of proteins BDNF, NT4, p75NTR, NGF & NT3 were identified as 0.627, 0.708, 0.367, 0.644 & 0.415. The results of molecular docking studies revealed among the selected ligands Methyl-ɣ-oresellinate, N-(4-Hydroxy-phenyl)-2-phenyl-N-phenylacetyl-acetamide, Atranorin and Oresellinate exhibited high binding affinity with selected protein. The key genes involved in Neurotrophin signaling pathway leading to ameloblastoma pathogenesis is revealed, which are closely associated with cell differentiation, cell proliferation, pro-apoptosis, and pro-survival regulations. Further it can be concluded that Neurotrophin signaling pathway could be one of the promising pathway to tailor the targeted drug therapy for Ameloblastoma treatment.

Keywords Ameloblastoma · Neurotrophin · Odontogenesis · Enrichment ontology analysis · Topology analysis · Leader genes · Molecular docking

✉ Sidhra Syed Zameer Ahmed
sidhrazameer@gmail.com

✉ Syed Zameer Ahmed Khader
zameerkhader@gmail.com

[1] Department of Biotechnology, K. S. Rangasamy College of Technology, K. S. R. Kalvinagar, Tiruchengode, Tamil Nadu 637 215, India

[2] Department of Oral & Maxillofacial Pathology and Microbiology, Vivekanandha Dental College for Women, Tiruchengode, Tamil Nadu, India

[3] Department of Oral & Maxillofacial Pathology and Microbiology, K. S. R. Institute of Dental Science and Research, Tiruchengode, Tamil Nadu, India

Abbreviations

MAPK	Mitogen-activated protein kinase
KEGG	Kyto Encylopedia of Genes and Genomics
STRING	Search Tool for the Retrieval of interacting Genes/Proteins
P13K-Akt	Phosphoinositide-3-kinase-protein kinaseB/Akt
BDNF	Brain Derived Neurotrophin Factor
NT4	Neurotrophin Factor 4
p75NTR	P75 neurotrophin receptor
NGF	Nerve Growth Factor
NT3	Neurotrophin-3
BRAF	V-Raf murine sarcoma viral oncogene homolog-B1
PPI	Protein–Protein Interaction

Published online: 10 June 2024

ANOVA	Analysis of variance
KW TEST	Kruskal Wallis Test
FDR	False Discovery Rate
CID	Compound ID
SDF	Structure Data File
PDB	Protein Data Bank
PDBQT	Protein Data Bank, Partial Change(Q),& Atom Type(T) format

Introduction

Ameloblastoma is a benign odontogenic tumor occurs in oral cavity, known for its highly destructive, and invasive behaviour with high recurrence rate. If left untreated, ameloblastoma often leads to extensive tissue destruction and deformity. Till date, surgery is considered as the treatment of choice which results in post-treatment compromised quality of life in the diseased. Ameloblastoma arises from the dysregulated molecular signalling of enamel producing or odontogenic rest cells, results in uncontrolled cell proliferation, tumor cell invasion and sometimes metastasis. The molecular basis of ameloblastoma is not completely explored and new molecular data are enhancing our knowledge of ameloblastoma pathology which may have relevant implications. The overexpression of the RAS–RAF–MAPK pathway is strongly allied with its pathology, through EGFR-mediated signalling or activating mutations in the BRAF gene. Targeting and inhibition of BRAF gene was the most recent advancement in the non-surgical treatment of ameloblastoma. Recent studies on ameloblastoma pathogenesis confirm that Neurotrophins and Neurotrophin receptors perform a significant role in ameloblastoma pathogenesis through (Masthan et al. 2015; Marin et al. 2021). Even though the involvement of the Neurotrophin signaling pathway in the pathogenesis of ameloblastoma is confirmed, the protein–protein interaction and protein regulation mechanisms are not yet clearly identified. Prediction of ameloblastoma pathogenesis involving protein will be useful to find new treatment methods as well as new therapeutic drugs for that target protein (Thomaz et al. 2020).

A comparative assessment of large-scale datasets of Protein–Protein Interaction (PPI) has also shown that in silico predictions of many interactions provided levels of accuracy close to those determined experimentally (Rao et al. 2014). Understanding how proteins interact in an integrated way in a cell to carry out cellular tasks depends on the identification of protein–protein relationships. PPIs play a role in the development of factors as well as in the proper functioning of specific proteins, determining vibrant cellular pathways. The relationship between protein multimeric complexes can be directly determined using PPI data (Ding et al. 2019) and the coordinated WNL (weighted Number of Links) score has predicted the leader gene. Utilizing the high-position functional classifications provided by the manually curated Kyoto Encyclopaedia of Genes and Genomes (KEGG) pathway chart (Abdelhalim et al. 2018) all sources of commercial justification are benchmarked and calibrated against prior knowledge. The process of clustering entails organizing comparable data in one cluster and various records in separate clusters. Among the many clustering algorithms available, K- Means and Fuzzy C- Means are two that are frequently employed, maybe as a result of their simplicity. Still, they bear a stoner to offer the number of clusters k as input (Walden et al. 2023).

Methodology

Retrieval of interacting genes and weighted number of link values

The main target receptors of ameloblastoma are retrieved from the Kyto Encyclopedia of Genes and Genomes (KEGG) pathway (https://www.genome.jp/kegg/) and the receptors related to homosapiens were retrieved using the Neurotrophin Signaling pathway or map04722 in the online server (Yoithapprabhunath et al. 2020) for further investigation. PPI networks are retrieved from the STRING V9.1 database (https://string-db.org/) for selected proteins where the STRING database exports the predicted protein interactions and active interaction sources with a confidence level of 0.900 (Szklarczyk 2014; Orlando 2013). From combined scores, WNL values were calculated using the formula = SUM (identical gene; end of identical gene × 1000) where, each gene's combined score generates a single value (Szklarczyk 2014).

K mean clustering algorithm

Genes are subsequently grouped (Cluster 1, Cluster 2, and Cluster 3) based on their WNL value using hierarchical or K-means algorithms (Leader genes were chosen based on higher WNL value), whereas Orphan genes are those that have no known interactions (WNL = 0) (Santos et al. 2016).

Statistical analysis

The statistical analysis for the clustered proteins by the k mean algorithm was carried out by Kruskal Walli's test a type of one way ANOVA with a significance of < 0.01 with WNL scores in different types of treatment by an online calculator using the link (https://www.socscistatistics.com/tests/kruskal/default.aspx) (Crow et al. 2019).

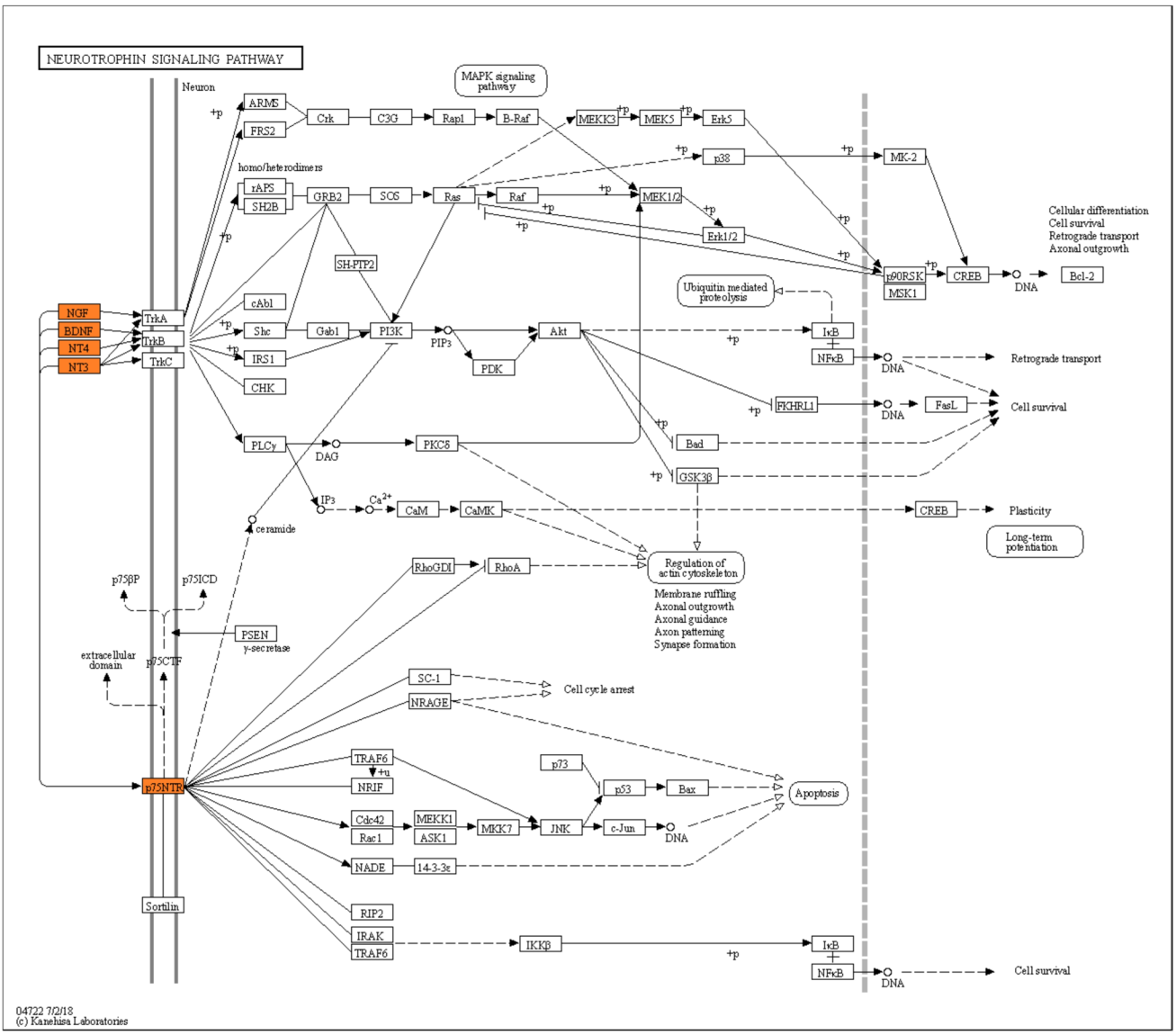

Fig. 1 Neurotrophin Signaling Pathway Retrieved from KEGG database

Enrichment analysis of the network

Ontology analysis was performed using ShinyGO software with significant pathways providing Network maps, Tree plots, cellular components, molecular functions, biological processes, and pathological phenomena for the protein retrieved from STRING software (Szklarczyk 2014). In subgroups, by promotor the enrichment FDR (False Discovery Rate) values revealed from which upregulated and downregulated proteins are calculated using formula [absolute log2 fold change, > 2; false-discovery rate (FDR), < 0.05] is used (Crow et al. 2019).

Topology analysis

Cytoscape 3.9.1v software was used to perform Network Enrichment analysis for developed PPI Network where cytoscape plugins "ClueGo" were used to calculate the topological properties especially clustering coefficient (Assenov 2008; Capriotti 2006).

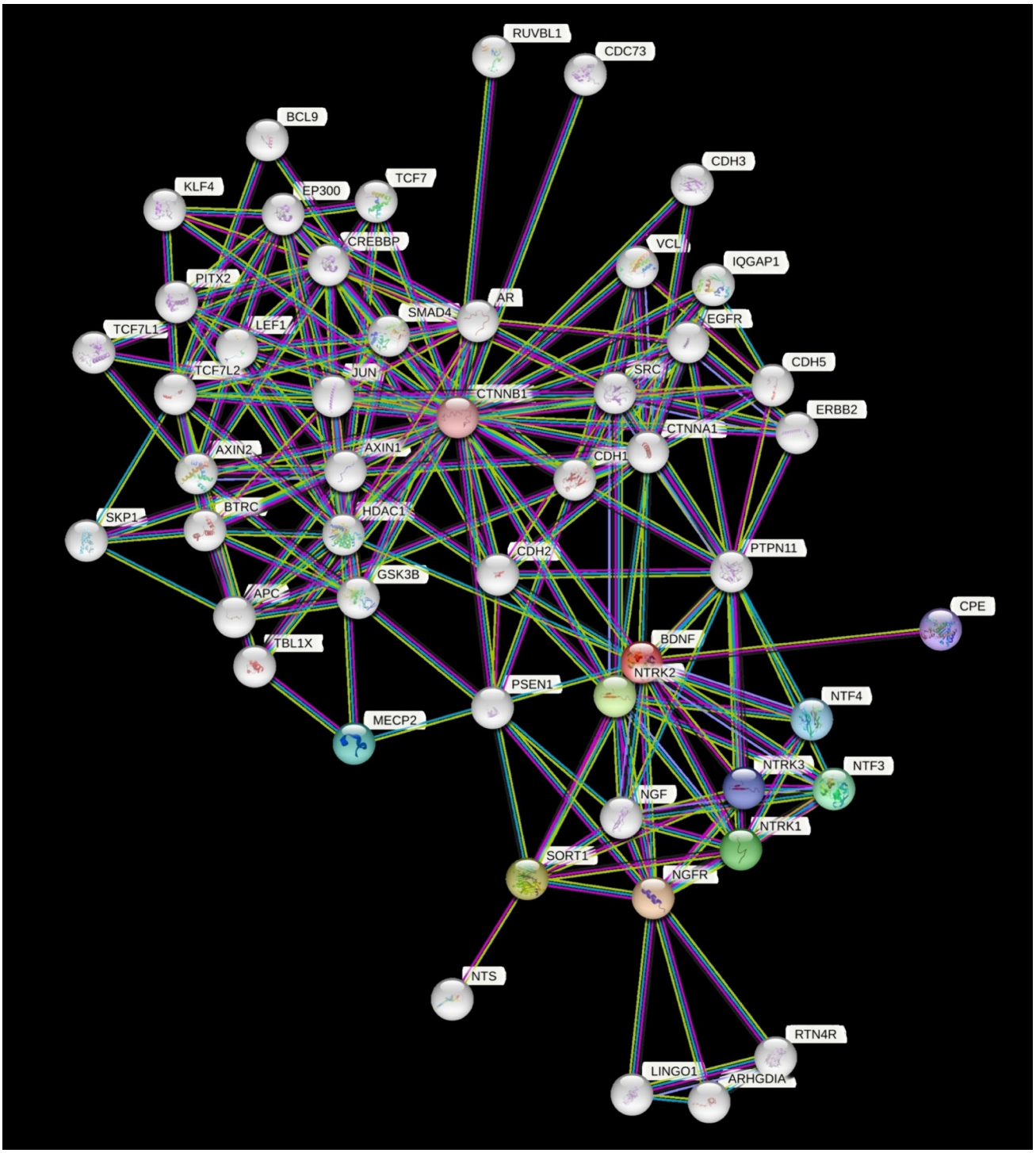

Fig. 2 String analysis for protein BDNF having 50 Nodes with Highest confidence of above 0.90

Molecular docking

Target protein and ligand retrieval

The proteins that make impact on Neurotrophin Signaling Pathway are initially identified (BDNF, NT4, p75NTR, NGF & NT3), retrieved from the Protein Data Bank (https://www.rcsb.org) in PDB format further converted to respective PDBQT format using Discovery visualizer tools. The polar hydrogen atoms were added to the receptor molecules prior to docking studies (Azmi et al. 2023).

Table 1 BDNF interacting proteins WNL value

GENES	WNL	GENES	WNL	GENES	WNL	GENES	WNL	GENES	WNL
CTNNB1	35,879	TCF7L2	10,602	BTRC	7821	VCL	4958	RTN4R	2900
BDNF	14,533	AR	9799	NTRK1	7791	NTF4	4869	LINGO1	2899
HDAC1	13,575	SMAD4	8912	SORT1	7784	IQGAP1	4855	ARHGDIA	2858
SRC	13,482	JUN	8809	APC	7783	PITX2	4768	TCF7L1	2857
PTPN11	13,441	AXIN1	8759	LEF1	7752	ERBB2	3980	BCL9	1986
CTNNA1	13,427	NGF	8715	EGFR	6954	TBL1X	3899	CDH3	1926
NGFR	11,885	CDH2	8644	NTF3	6846	KLF4	3849	CDC73	999
NTRK2	11,588	CDH1	7959	PSEN1	6795	SKP1	3817	NTS	999
CREBBP	11,475	GSK3B	7934	CDH5	5807	TCF7	3774	RUVBL1	999
EP300	10,751	AXIN2	7843	NTRK3	5796	MECP2	2959	CPE	984

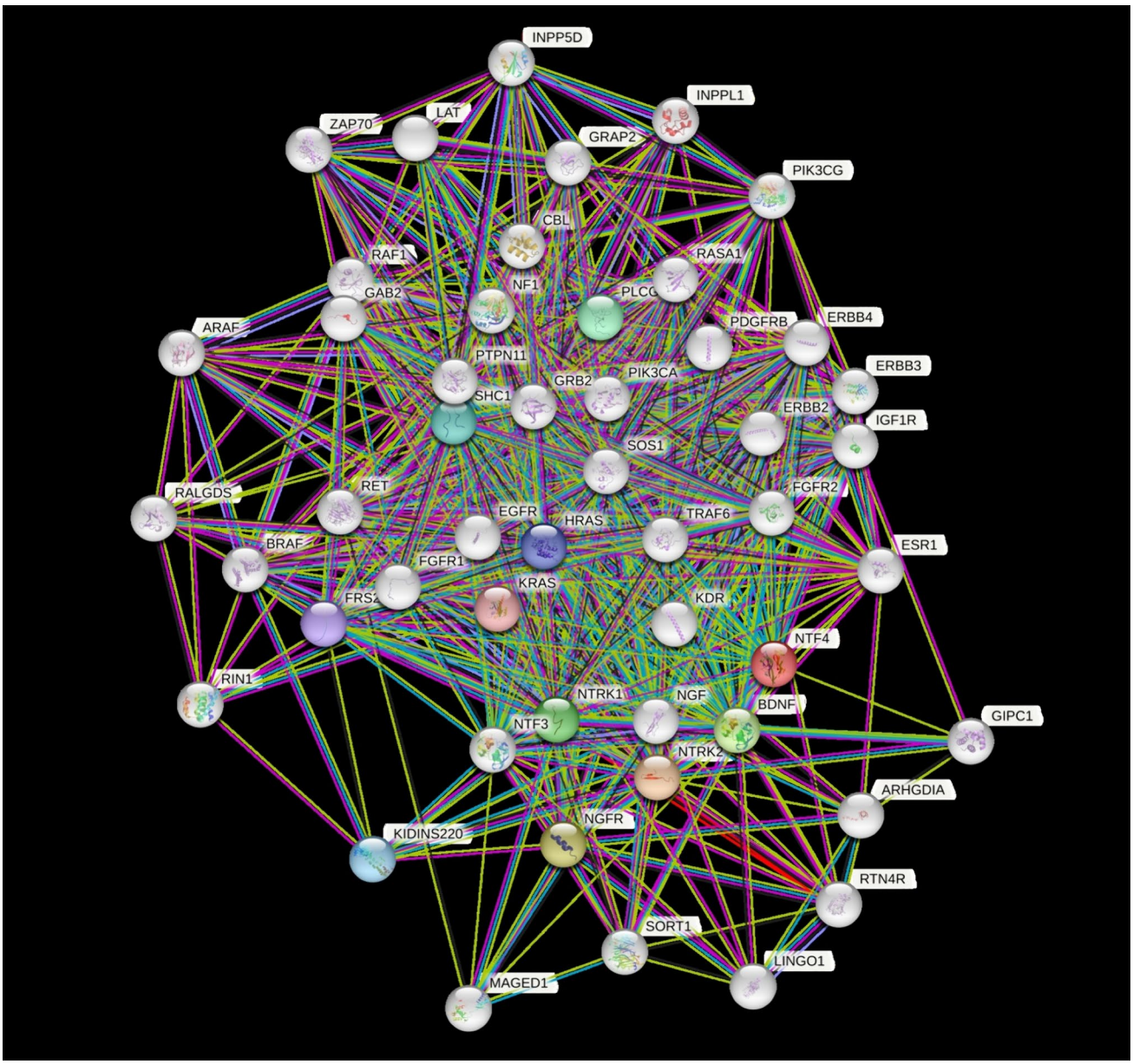

Fig. 3 String analysis for protein NT4 having 50 Nodes with Highest confidence of above 0.90

Table 2 NT4 interacting proteins WNL value

GENES	WNL	GENES	WNL	GENES	WNL	GENES	WNL	GENES	WNL
HRAS	25,304	NGF	1239	INPP5D	7539	MET	4864	SHC1	1997
EGFR	20,694	ERBB3	1069	NTF3	7511	ARAF	4837	RAF1	1946
GRB2	20,579	FGFR2	9723	NTF4	7468	LAT	4799	RET	1946
BDNF	19,915	ERBB4	9608	GRAP2	6789	GIPC1	4753	RASA1	189
CBL	19,622	NTRK1	8547	ESR1	6736	KIDINS220	4741	PIK3G	1853
KRAS	18,415	FGFR1	7786	PIK3A	6606	BRAF	3943		
GAB1	18,021	PDGFB	7758	KDR	581	INPPL1	3836	RTN4	999
FRS2	14,474	IRS1	7736	NTRK2	5799	MAGED1	3829	PTPN2	997
NGFR	12,719	GAB2	7717	FLT4	5777	LINGO1	2968	RIPK2	988
ERBB2	12,712	IGF1R	771	PTPN1	5705	ARHGDIA	2858	SORT1	926

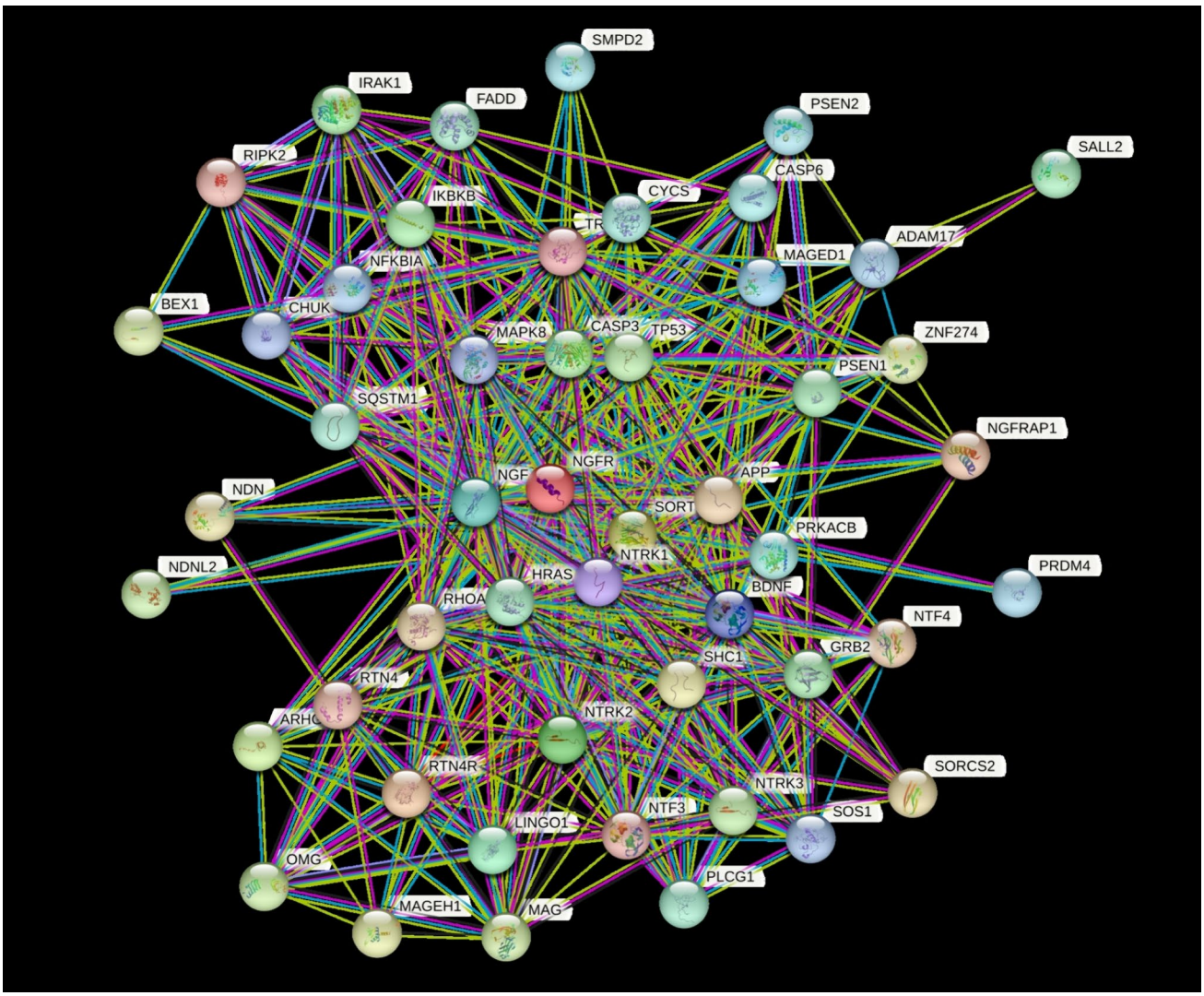

Fig. 4 String analysis for protein p75NTR having 50 Nodes with Highest confidence of above 0.90

Table 3 p75NTR interacting proteins with WNL value

GENES	WNL	GENES	WNL	GENES	WNL	GENES	WNL	GENES	WNL
NGFR	47,144	HRAS	12,390	NTF4	9467	FADD	5750	NGFRAP1	3778
NGF	33,913	SOS1	12,223	CASP3	8604	PSEN1	5720	PSEN2	3771
SORT1	19,647	MAPK8	11,343	SQSTM1	8552	MAGED1	5642	BEX1	3713
TRAF6	19,182	PLCG1	10,618	RIPK2	8478	RTN4	4948	MAGEH1	2870
BDNF	18,129	NTF3	10,501	ZNF274	8284	MAG	4894	NDNL2	2772
NTRK1	17,310	TP53	10,436	RTN4R	7789	OMG	4821	SMPD2	2766
SHC1	14,613	APP	9745	NFKBIA	7673	CYCS	4686	PRDM4	2760
GRB2	13,480	NTRK3	9605	IRAK1	7666	ADAM17	4584	PRKACB	2755
NTRK2	12,622	IKBKB	9600	LINGO1	6783	ARHGDIA	3857	SORCS2	1920
RHOA	12,472	CHUK	9543	CASP6	6593	NDN	3856	SALL2	940

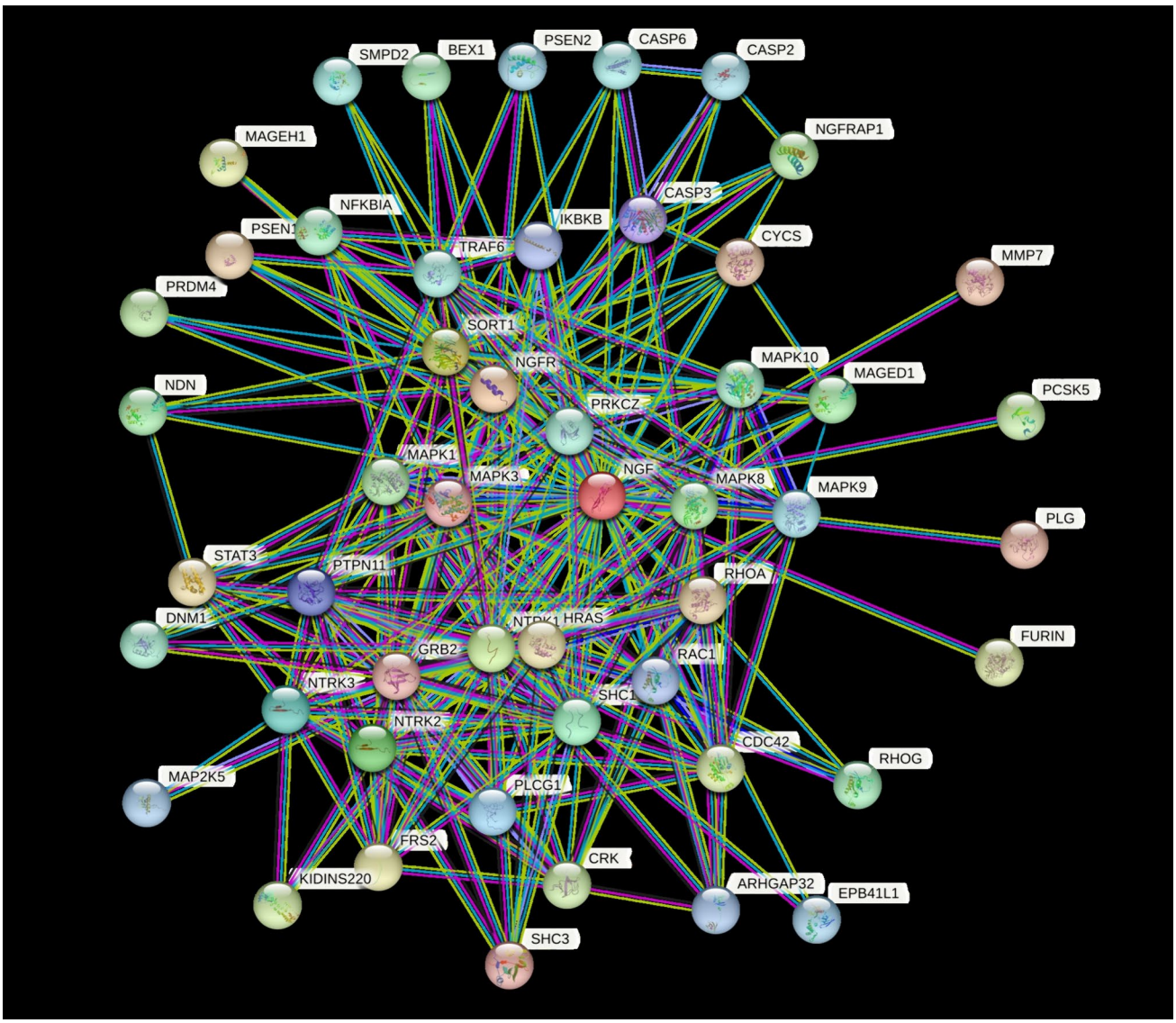

Fig. 5 String analysis for protein NGF having 50 Nodes with Highest confidence of above 0.90

Table 4 NGF interacting proteins with WNL value

GENES	WNL	GENES	WNL	GENES	WNL	GENES	WNL	GENES	WNL
NGF	46,412	MAPK8	15,171	CRK	10,431	IKBKB	5706	PSEN2	2801
NGFR	29,496	RAC1	14,992	MAPK10	10,154	NGFRAP1	4724	SMPD2	2766
NTRK1	25,673	PTPN11	14,521	STAT3	9560	CASP2	4668	PRDM4	2760
GRB2	1846	RHOA	1442	CASP3	8585	DNM1	4657	RHOG	2758
SORT1	16,807	TRAF6	13,336	PLCG1	7796	CASP6	4651	MAP2K5	1843
SHC1	1645	PRKCZ	13,081	MAGED1	7449	KIDINS220	3852	EPB41L1	1828
MAPK1	16,269	CDC42	11,523	NFKBIA	6689	PSEN1	3819	PLG	958
MAPK3	15,483	NTRK3	11,385	CYCS	6600	NDN	3769	MMP7	954
NTRK2	15,447	MAPK9	11,149	ARHGAP32	5739	MAGEH1	2870	FURIN	946
HRAS	15,277	FRS2	10,742	SHC3	5734	BEX1	2808	PCSK5	941

Three-dimensional affinity grids were created at the geometric centers of the target proteins.

Whereas the Ligand molecules (3D structure) were retrieved from PubChem database (https://pubchen.ncbi.nlm.nih.gov) as SDF format by searching its Compound ID (CID) number. **C1-** N-(4-Hydroxy-phenyl)-2-methoxy-2-phenyl-acetamide (CID-55037379); **C2-** N-(4-Hydroxy-phenyl)-2-phenyl-N-phenylacetyl-acetamide (CID-138708358); **C3-** Methyl-ɣ-oresellinate (CID-76658); **C5-** Atranorin (CID-68066); **C6-** Usnic Acid (CID- 5646); **C7**- Oresellinate (CID- 54,718,175); **C8-** 2-Hydroxy(Masthan et al. 2015; Rao et al. 2014) naphthoquinone (CID-6755); **C9-** N-Benzoyl-4-hydroxy-benzamide (CID- 364,849); **C10-** Fingolimod (standard drug) (CID-107970) (Syed et al. 2021; Syed et al. 2023a, b; Thangakumar et al. 2019) and optimized using Discovery Studio (Ragunathan et al. 2022).

Molecular docking for selected proteins and ligands

The energy-optimized structure of ligands were docked with target proteins using Auto Dock Vina 1.1.2 (Trott et al. 2010). Compound interaction was characterized by the protein's affinity for the receptor and the target PBD molecules were loaded, transformed into PDBQT using PyRx's Auto dock application (Forli et al. 2016).

Discovery studio visualizer

The Docked PyRX results were visualized and analyzed using Discovery Studio Visualizer, and the results were downloaded as 2D image.

Molecular dynamic simulations

The target proteins were minimized using the GROMACS software. CHARMM36 force field and TIP3P water model were used for the solvation process. System charges were balanced with ions. The CHARMM36 force field minimized the system energy, with SHAKE program ensuring water molecule symmetry and bond length. Initially, the system was energy minimized using the steepest descent method and simulation were done at a constant temperature of 300 K under NPT conditions for 100 ns. This equilibration techniques ensures a stable starting point for molecular dynamic simulations of proteins, enabling accurate structural and dynamic behavior of protein.

Results

Retrieval of interacting genes

From the previous study on the pathogenesis of ameloblastoma, it is found that Neurotrophin signaling pathway plays a predominant role where different genes and different proteins were involved. From KEGG (Kyto Encylopedia of Genes and Genomes) database the proteins that are involved in the Neurotrophin signaling pathway were retrieved as high-resolution image Fig. 1.

Protein–protein interaction (PPI) analysis using STRING tool

The Protein–Protein Interaction (PPI) analysis is done using STRING database where the selected proteins BDNF, NT4, p75NTR, NT3 and NGF are given as inputs. The parameters were selected with High confidence of > 0.90 and 50 number of nodes. The proteins interacting with BDNF were retrieved (Fig. 2) with top 50 proteins are shown in Table 1 and reveals the WNL values of BDNF interacting proteins and CTNNB1, BDNF, HDAC1, SRC, PTPN11, CTNNA1, NGFR, NTRK2, CREBBP and EP300 were recognized as leader genes.

Similarly, results of NT4 expressed high level of interaction with highest confidence of above 0.90 (Fig. 3) and the WNL values of NT4 interacting proteins were reported in

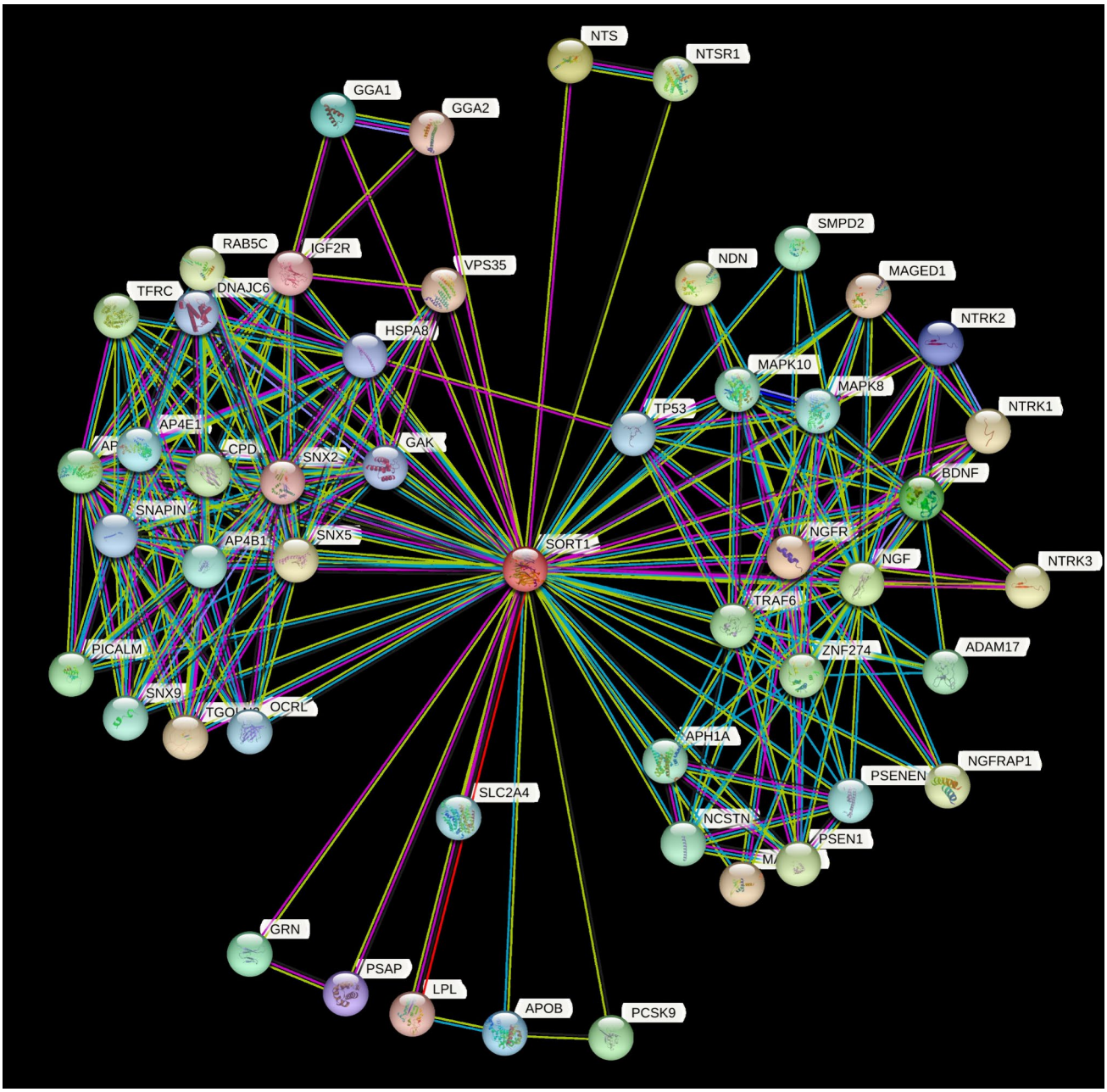

Fig. 6 String analysis for protein NT3 having 50 Nodes with Highest confidence of above 0.90

Table 2 with leader genes HRAS, EGFR, GRB2, BDNF, CBL, KRAS, GAB1, FRS2, NGFR and ERBB2.

The results of p75NTR explored better interaction with top 50 proteins (Fig. 4). From these 50 proteins NGFR, NGF, SORT1, TRAF6, BDNF, NTRK1, SHC1, GRB2, NTRK2 and RHOA were identified as leader genes with higher weighted number of links (Table 3).

Figure 5 demonstrates the interaction of NGF with proteins with highest confidence are represented. Through WNL values (Table 4) NGFR, NGF, NTRK1, GRB2, SORT1, SHC1, MAPK1, MAPK3, NTRK2 and HRAS were expressed as leader genes.

NT3 showed higher interactions with proteins having highest confidence of above 0.90 (Fig. 6). The WNL values for NT3 interacting proteins were displayed in Table 5 from which SORT1, NGFR, NGF, SNX2, SNX5, AP4E1, AP3B1, AP4B1, CPD and SNAPIN were identified as leader genes.

Table 5 NT3 interacting proteins WNL value

GENES	WNL	GENES	WNL	GENES	WNL	GENES	WNL	GENES	WNL
SORT1	45,969	TRAF6	13,117	TFRC	8319	PICALM	7302	MAGEH1	2870
NGFR	20,188	HSPA8	12,121	MAPK10	8235	NTRK1	6706	NGFRAP1	2869
NGF	17,961	ZNF274	11,886	RAB5C	8233	NTRK2	4879	SMPD2	2766
SNX2	16,764	BDNF	11,463	PSEN1	7718	VPS35	4854	NTS	1998
SNX5	16,735	IGF2R	10,548	TGOLN2	7536	ADAM17	4584	GRN	1956
AP4E1	15,870	GAK	10,190	NCSTN	7534	NDN	3856	LPL	1949
AP3B1	15,669	DNAJC6	9225	APH1A	7528	NTRK3	385	PSAP	1943
AP4B1	15,581	TP53	8602	PSENEN	7527	GGA1	2979	NTSR1	1929
CPD	15,491	MAGED1	8512	SNX9	7355	APOB	2942	PCSK9	1882
SNAPIN	15,449	MAPK8	8373	OCRL	7303	GGA2	2936	SLC2A4	910

Table 6 Cluster analysis of proteins

Protein	Clusters	Protein name
BDNF	Cluster 1 (35 proteins)	APC, AR, AXIN1, AXIN2, BCL9, BTRC, CDC73, CDH1, CDH2, 5CDH3, CDH5, CREBBP, CTNNA1, CTNNB1, EGFR, EP300, ERBB2, GSK3B, HDAC1, IQGAP1, JUN, KLF4, LEF1, PITX2, PSEN1. PTPN11, RUVBL1, SKP1, SMAD4, SRC, TBL1X, TCF7, TCF7L1, TCF7L2 and VCL
	Cluster 2 (11 proteins)	NGFR, NTRK2, NTRK1, NGF, NTF3, SORT1, BDNF, NTRK3, NTF4, MECP2 and CPE;
	Cluster 3 (3 proteins)	ARHGDIA, LINGO1 and RTN4R
NT4	Cluster 1 (17 proteins)	CBL, EGFR, ERBB2, ERBB3, ESR1, GAB2, GRAP2, GRB2, INPPL1, KRAS, LINGO1, PLCG1, PTPN11, RASA1, SHC1, SOS1 and ZAP70
	Cluster 2 (20 proteins)	HRAS, PIK3CA, RAF1, NF1, PIK3CG, KDR, PDGFRB, ARAF, FGFR1, RALGDS, BRAF, ERBB4, RET, FGFR2, IGF1R, INPP5D, NTRK2, LAT, R1N1 and ARHGDIA
	Cluster 3 (13 proteins)	NTRK1, BDNF, NGF, NGFR, SORT1, NTF3, NTF4, KIDINS220, TRAF6, FRS2, MAGED1, RTN4R and GIPC1
p75NTR	Cluster 1 (9 proteins)	APP, GRRB2, HRAS, NTRK1, NTRK2, NTRK3, PLCG1, SHC1 and SOS1
	Cluster 2 (29 proteins)	ARHGDIA, BDNF, BEX1, CASP3, CASP6, CYCS, LINGO1, MAG, MAGED1, MAGEH1, NDN, NDNL2, NGF, NGFR, NGFRAP1, NTF3, NTF4, OMG, PRDM4, PRKACB, RHOA, RIPK2, RTN4, RTN4R, SALL2, SMPD2, SORCS2, SORT1 and ZNF274
	Cluster 3 (12 proteins)	ADAM17, CHUK, FADD, IKBKB, IRAK1, MAPK8, NFKBIA, PSEN1, PSEN2, SQSTM1, TP53 and TRAF6
NGF	Cluster 1 (9 proteins)	IKBKB, MAPK8, MAPK9, NFKBIA, NGFR, PRKCZ, PSEN1, PSEN2 and TRAF6
	Cluster 2 (28 proteins)	ARHGAP32, BEX1, CASP2, CASP3, CASP6, CRK, CYCS, EPB41L1, FURIN, KIDINS220, MAGED1, MAGEH1, MAP2K5, MAPK10, MMP7, NDN, NGF, NGFRAP1, NTRK1, NTRK2, NTRK3, PCSK5, PLG, PRDM4, RAC1, RHOG, SMPD2 and SORT1
	Cluster 3 (13 proteins)	CDC42, DNM1, FRS2, GRB2, HRAS, MAPK1, MAPK3, PLCG1, PTPN11, RHOA, SHC1, SHC3 and STAT3
NT3	Cluster 1 (17 proteins)	ADAM17, BDNF, MAGED1, MAGEH1, MAPK8, NDN, NGF, NGFR, NGFRAP1, NTRK1, NTRK2, NTRK3, PSEN1, PSENEN, SMPD2, TRAF6 and ZNF274
	Cluster 2 (27 proteins)	AP3B1, AP4B1, APH1A, APOB, CPD, GGA1, GGA2, GRN, IGF2R, LPL, MAPK10, NCSTN, NTS, NTSR1, OCRL, PCSK9, PICALM, PSAP, RAB5C, SLC2A4, SNAPIN, SNX2, SNX5, SNX9, SORT1, TGOLN2 and VPS35;
	Cluster 3 (6 proteins)	AP4E1, DNAJC6, GAK, HSPA8, TFRC and TP53

K mean clustering & statistical analysis

K mean clustering was carried out for all five selected proteins, leads to categorization of interacting proteins into three clusters for each protein based on unsupervised learning algorithm represented in Table 6 for protein BDNF, NT4, p75NTR, NGF, NT3.

The clustered interacting proteins are ranked based on their WNL values and Kruskal Walli's test for each selected protein cluster. For protein BDNF, NT4, p75NTR and NGF network forms three clusters that equally contributes in the metabolic pathway which showed significant result in KW's test with a P-value of 0.00152, 0.00111, 0.00278 and 0.00833 for BDNF, NT4, p75NTR and NGF (below selected P-value 0.01). The Protein NT3 network forms three clusters

Table 7 Protein regulation by query protein BDNF, NT4, p75NTR, NGF and NT3 in upregulated protein

GENE	P val	FDR	GENE	P val	FDR
ZNF202	0.00000572	0.00237	MZF1	0.00041	0.03411
MZF1	0.0000315	0.01303	NHLH1	0.00041	0.03411
PATZ1	0.0000683	0.01414	PATZ1	0.00063	0.04331
MZF1	0.000134	0.01852	EGR1	0.00073	0.04331
MZF1	0.000304	0.03148	KLF5	0.000202	0.00959
CGBP	0.000409	0.03389	EGR4	0.00016	0.02763
NHLH1	0.000595	0.03877	SP1	0.0002	0.02763
EGR1	0.00066	0.03877	PATZ1	0.00042	0.0355
ZNF202	0.000749	0.03877	TFAP2A	0.00043	0.0355
MZF1	0.000405	0.0075	ZNF263	0.00057	0.03736
KLF5	0.000202	0.03411	MLL	0.00063	0.03736
SP1	0.000373	0.03411	MZF1	0.000022	0.0093

that unequally contribute in the metabolic pathway, which shows a result of 0.14839 (above selected P-value 0.01) that indicates the protein network of NT3 is not significant across clusters. Thus the table value is greater than the calculated value for NT3 (Table 7).

Enrichment analysis of network

The signalling mechanism associated with query protein and other signalling mechanisms that gets activated are identified by GO software, followed by identification of Upregulated and downregulated by ontology analysis. Enriched promotor p-value, network map, tree plots and signalling pathway charts were obtained as results from ShinyGO software. Figure 7 represents BDNF tree plot and interacting network, where Fig. 7a demonstrates the role of BDNF in Cell surface receptor signalling pathway, regulation of cell differentiation and regulation of the development process with an FDR (False Discovery Rate) value of 9.6e-29, 6.3e-25 and 5.2e-24. The interaction map of NGF protein is represented in Fig. 7b.

Figure 8 explores NT4 tree plot and interaction map, in which Fig. 8a reveals the major involvement of NT4 in Neurotrophin signaling pathway, proteoglycans in cancer, EGFR tyrosine kinase inhibitor resistance, MAPK signaling pathway, PI3K-Akt signaling pathway and Ras signaling pathway with a FDR value of 2.7e-38, 2.0e-27, 4.3e-29, 5.0e-33, 4.4e-31 and1.2e-37.

The p75NTR tree plot and interaction map is represented in Fig. 9a, b, where Fig. 9a reveals the major involvement of p75NTR in Neurotrophin signaling pathway with a FDR value of 1.1e-21 as well as in Ras signaling pathway and MAPK signaling pathway with FDR value of 2.3e-13 & 2.3e-10. Figure 10a reveals the major involvement of NGF in Neurotrophin signaling pathway with a FDR value of 2.7e-19 as well as with Ras signaling pathway, PI3K-Akt signaling pathway and MAPK signaling pathway with FDR value of 5.6e-14, 2.3e-10 and 8.2e-11 and Fig. 10b reveals the pathway interaction map.

Figure 11a reveals the major involvement of NT3 in Neurotrophin TRK receptor signaling pathway, Membrane protein intracellular domain proteolysis, Post regulation of programmed cell death, Post regulation of cell death,

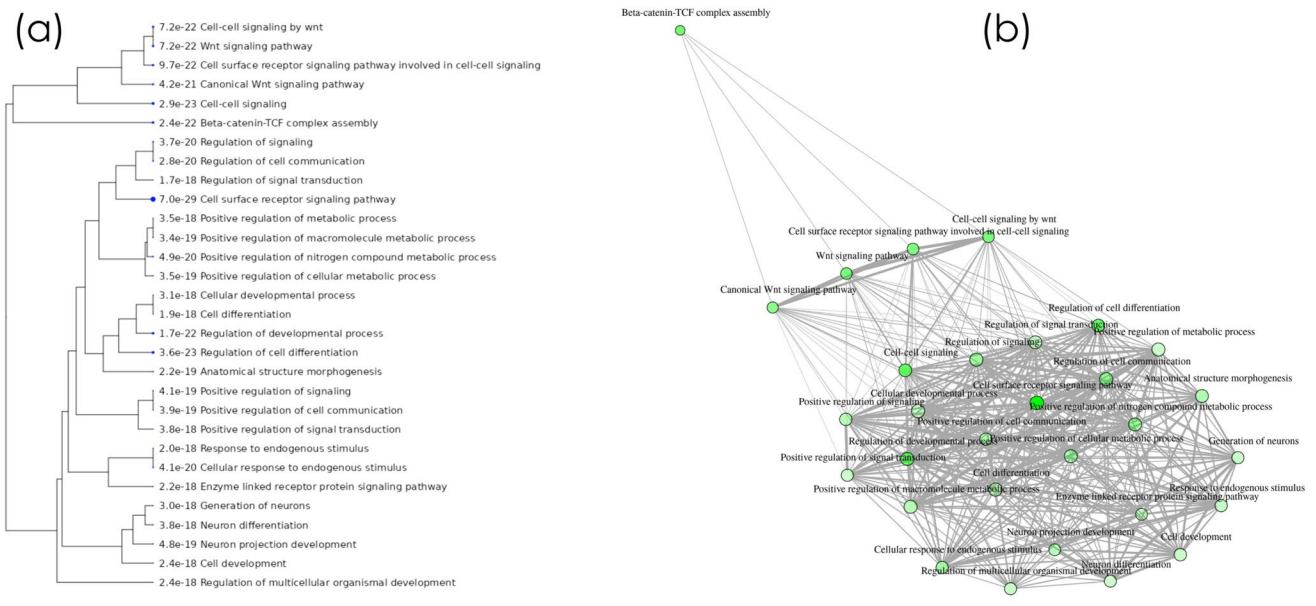

Fig. 7 BDNF Tree plot and Interacting network by ShinyGO

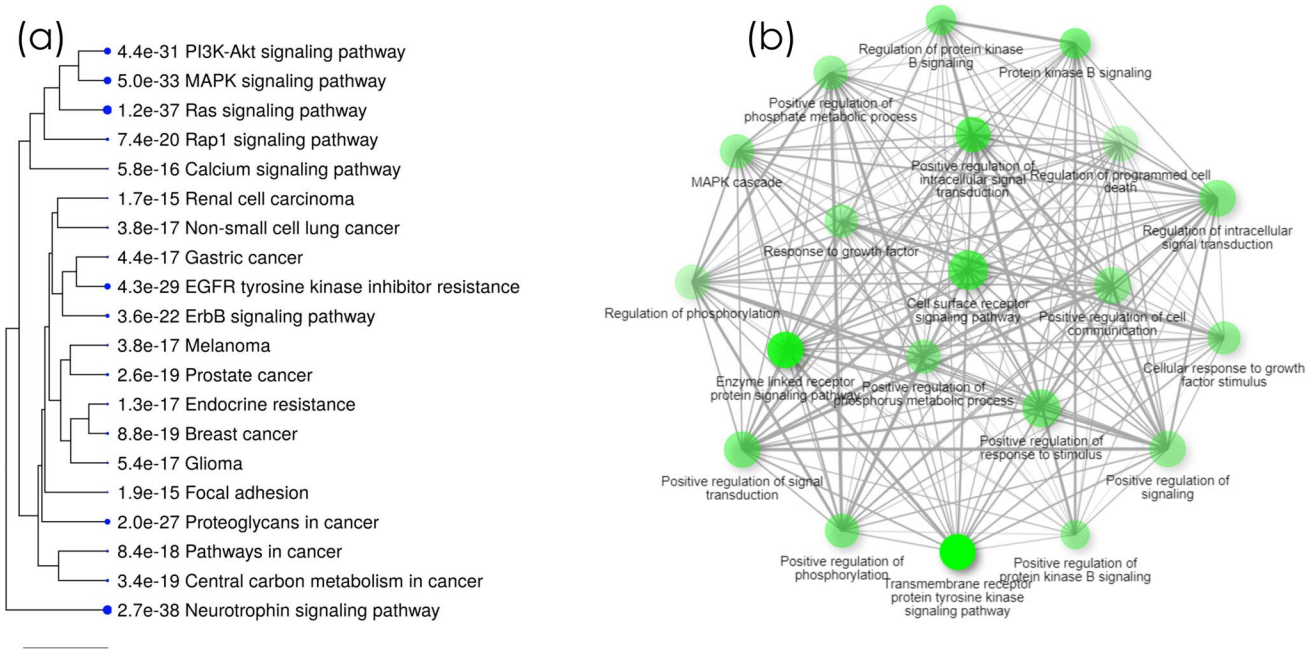

Fig. 8 NT4 Tree plot and Interacting network by ShinyGO

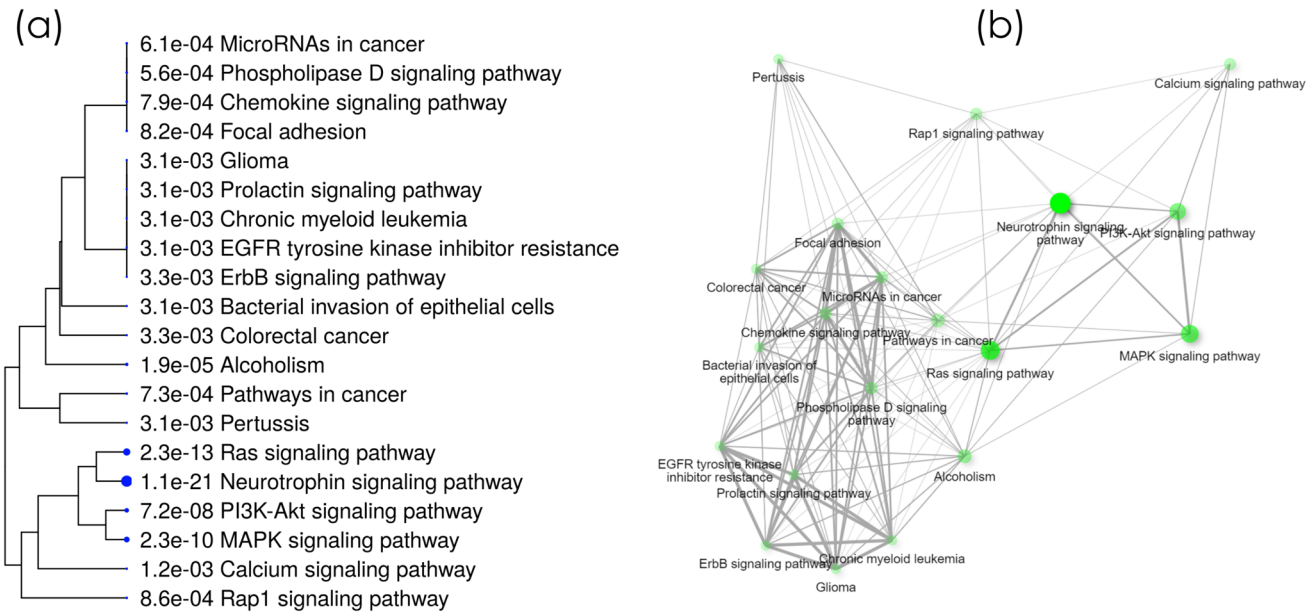

Fig. 9 p75NTR Tree plot and Interacting network by ShinyGO

Regulation of cell death and lysosome transport with a FDR value of 2.5e-10, 1.7e-11, 8.7e-11, 6.4e-11, 2.1e-10 and 8.7e-11; Fig. 11b reveals the pathway interaction map. Unlike p75NTR and NGF the NT3 protein mainly interacts with Lysosome pathway and Endocytosis.

Topology analysis

The Topology analysis was performed to identify the Clustering Coefficient value which reviling the highest possible interlinkage of query protein with other genes in the network and the parameters are depicted in Table 8. In this, the Clustering coefficient value mainly express the highest possible interlinkage by query protein; clustering coefficient

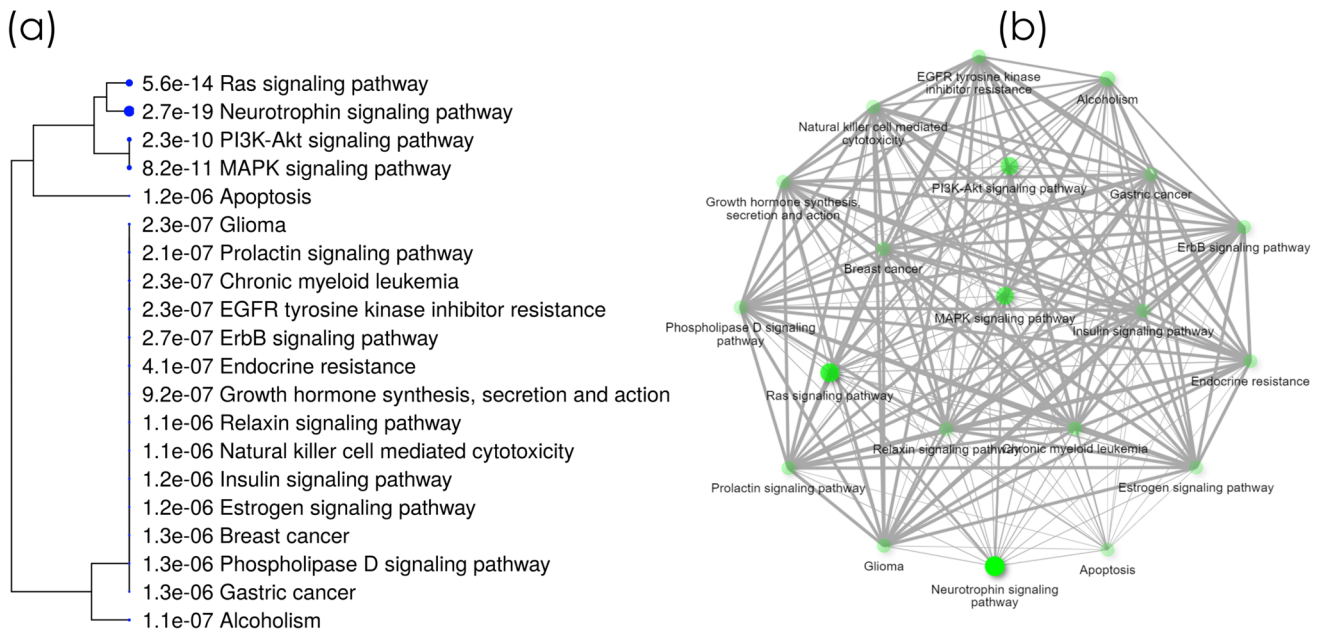

Fig. 10 NGF Tree plot and Interacting network by ShinyGO

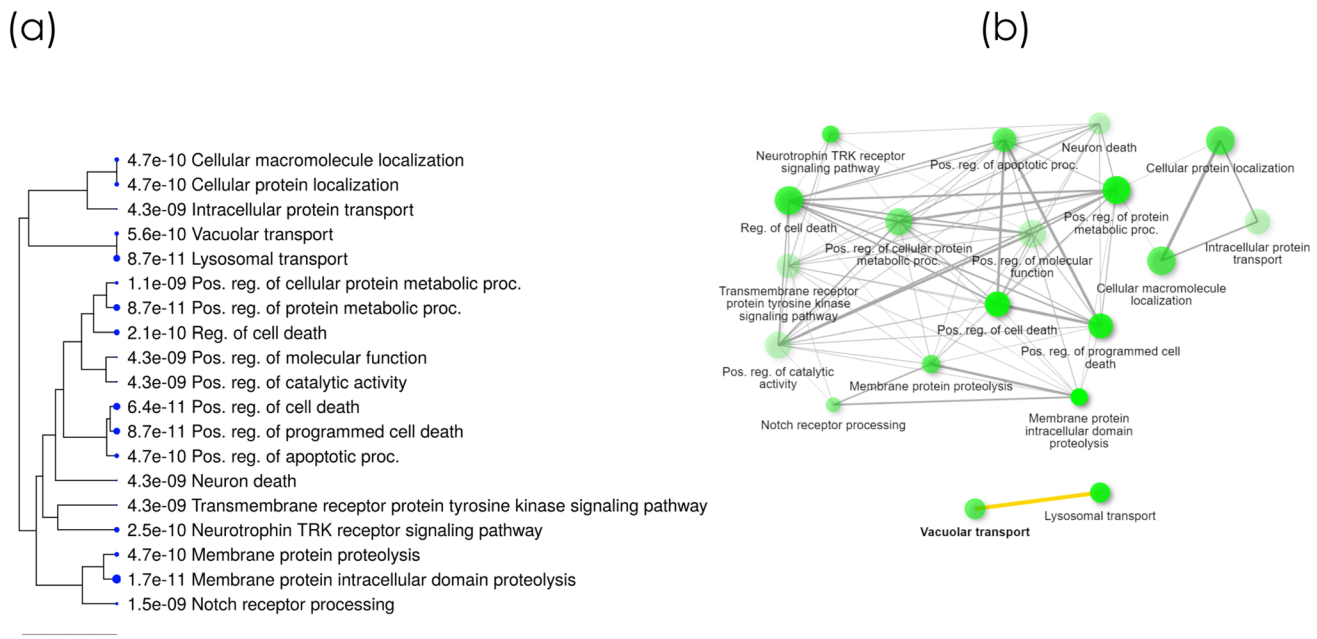

Fig. 11 NT3 Tree plot and Interacting network by ShinyGO

value for BDNF, NT4, p75NTR, NGF and NT3 are 0.627, 0.708, 0.367, 0.644 and 0.415. Among the genes NT4, NGF and BDNF represents high degree of interlinkage with its network proteins.

Molecular docking

The selected targeted proteins are 1. Brain-Derived Neurotrophic Factor (SLASH) & Neurotrophin 3—Heterodimer (PDB ID: 1BND), 2. Neurotrophin 4—Homodimer (PDB ID: 1B98), 3. Neurotrophin 3- from Human (PDB ID: 1B8K), 4. NGF in Complex with Domain 5 of the Trka

Table 8 Topology analysis of p75NTR by Cytoscape software

Parameter	BDNF	NT4	p75NTR	NGF	NT3
Number of nodes	50	50	50	50	50
Number of edges	740	858	247	510	235
Avg. number of neighbors	14.800	13.120	9.88	10.2	9.4
Network diameter	2	3	4	2	3
Network radius	1	2	1	1	1
Characteristic path length	1.694	1.950	1.726	1.793	1.561
Clustering coefficient	0.627	0.708	0.367	0.644	0.415
Network density	0.302	0.393	0.101	0.208	0.096
Connected components	1	1	1	1	1
Multi-edge node pairs	370	328	0	255	0
Number of self-loops	0	0	0	0	0
Analysis time (sec)	0.156	0.235	0.126	0.141	0.063

Receptor (PDB ID: 1WWW) and 5. Neurotrophin-3 & p75NTR Symmetrical Complex (PDB ID: 3BUK) downloaded as PDB format and energy minimization analysis was performed using steepest descent method (Table 9).

The selected biomolecules are represented with compounds Name, CID, molecular formula and molecular Weight (Table 8) possessing favorable ADME (absorption, distribution, metabolism, and excretion), Physiochemical, Pharmacokinetics and Drug likeliness properties which are shown in Supplementary file (Table S1–S3). Molecular docking is performed for proteins BDNF, NT4, p75NTR, NGF, and NT3 with 10 selected ligands; As a result, 12 ligands disclosed notable interaction with a binding affinity value below − 7 (kcal/mol) (Table 10) were selected for further visualization.

Figure 12 reveals 4 sets of molecular interactions with selected ligands, whereas Fig. 12a indicates BDNF—C7 complex showing a binding affinity score of − 7 (kcal/mol) forms interaction due to the binding of ligand with amino

Table 9 Ligand Molecules

S. no	Compound name	CID number	Formula	Molecular weight
1	**C1-** N-(4-Hydroxy-phenyl)-2-methoxy-2-phenyl-acetamide	55,037,379	$C_{15}H_{15}NO_3$	257.3 g/mol
2	**C2-** N-(4-Hydroxy-phenyl)-2-phenyl-N-phenylacetyl-acetamide	138,708,358	$C_{22}H_{19}NO_3$	345.4 g/mol
3	**C3-** Methyl-ɣ-oresellinate	76,658	$C_9H_{10}O_4$	182.17 g/mol
4	**C4-** Roccellatol	139,591,667	$C_{12}H_{16}O_7$	272.25 g/mol
5	**C5-** Atranorin	68,066	$C_{19}H_{18}O_8$	374.3 g/mol
6	**C6-** Usnic acid	5646	$C_{18}H_{16}O_7$	344.3 g/mol
7	**C7**- Oresellinate	54,718,175	$C_8H_7O_4$	167.14 g/mol
8	**C8-** 2-Hydroxy(Masthan et al. 2015; Rao et al. 2014) naphthoquinone	6755	$C_{10}H_6O_3$	174.2 g/mol
9	**C9-** N-Benzoyl-4-hydroxy-benzamide	364,849	$C_{14}H_{11}NO_3$	241.2 g/mol
10	**C10-** Fingolimod (standard drug)	107,970	$C_{19}H_{33}NO_2$	307.5 g/mol

Table 10 Interacting amino acids and Binding affinity of Protein–Ligand Complex

Figure	Protein–ligand complex	Interacting amino acids	Binding affinity (Kcal/Mol)
a	**BDNF–C7**	TRP 76, ILE 70, VAL 63, GLY 69, LYS 64	− 7
b	**BDNF–C9**	CYS108, VAL 110, THR 112, CYS 14, SER 16, TYR 53	− 7.3
c	**NT4–C3**	AGR 27, GLU 58, VAL 24, ARG 28, THR 29, VAL 31	− 10.4
d	**NT4–C4**	LEU 33, TRP 112, TRP 23, TYR 55	− 7.1
e	**NT3–C5**	TYR 53, VAL 86, TYR 51, LYS 49	− 7
f	**NGF–C2**	HIS 353	− 8.7
g	**NGF–C5**	PHE 101, PRO 382, TYR 52, TRP 21, LYS 88, LYS 50, VAL 48	− 7
h	**p75NTR–C1**	VAL 141, LYS 73, VAL 141, CYS 139, ASP 71, LYS 73	− 7.3
i	**p75NTR–C2**	ASP 15, VAL 133, LYS 58	− 7.6
j	**p75NTR–C4**	ASP 71, ASP 72, THR, 140, LYS 73, VAL 141	− 7.8
k	**p75NTR–C5**	ASP 72, THR 140, HIS 74, LYS 73, VAL 141, ASP 71, PRO 138	− 8.5
l	**p75NTR–C7**	ARG 68, SER 12, SER 16, TYR 83, GLY 84	− 8

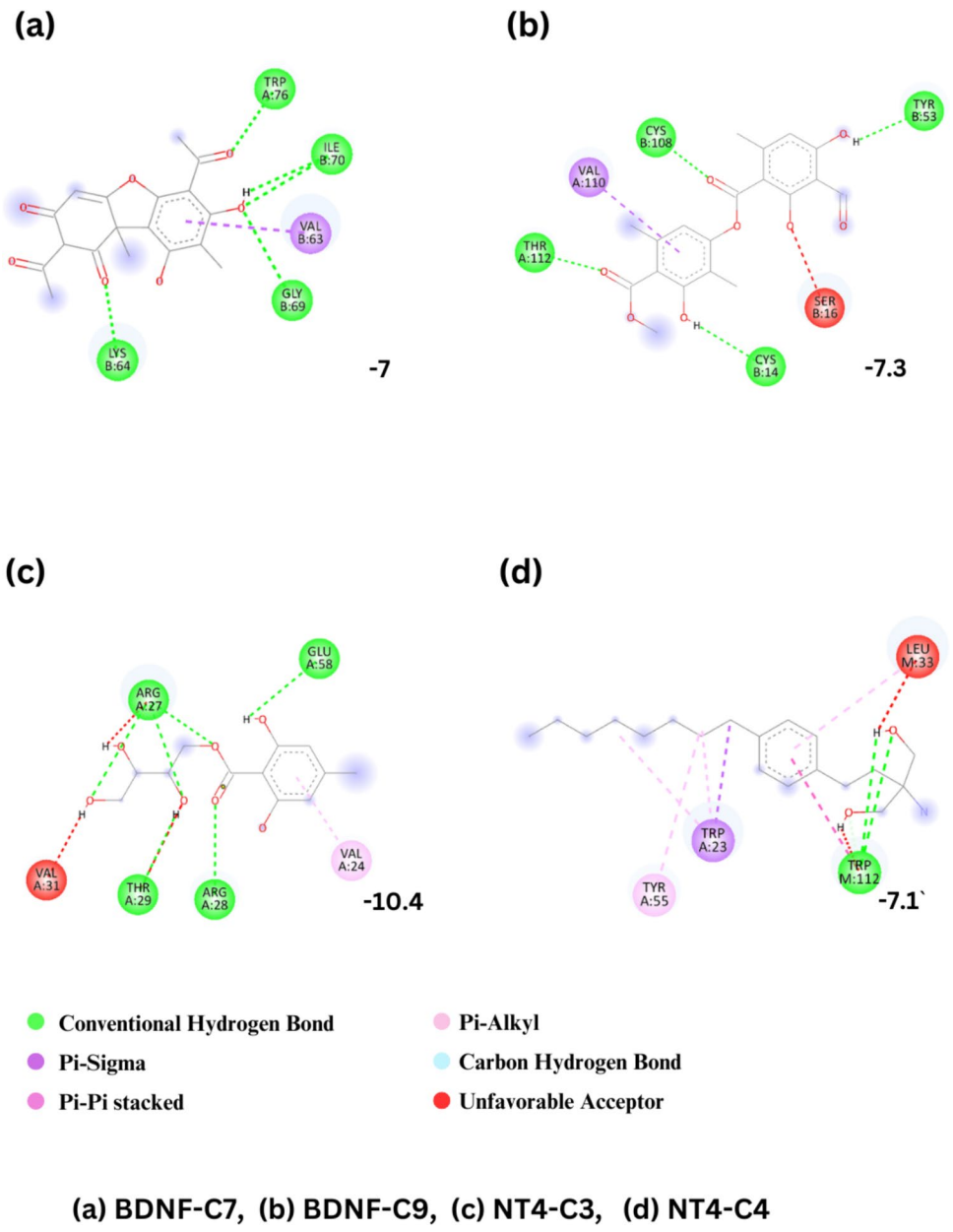

Fig. 12 Visualized molecular docking interacting complexes; **a** BDNF-C7, **b** BDNF-C9, **c** NT4-C3 & **d** NT4-C4

acids in protein active sites. Figure 12b represents BDNF—C9 complex with active sites and a binding affinity score of − 7.3 (kcal/mol). NT4—C3 complex was denoted Fig. 12c with binding pockets and a binding affinity score of − 10.4 (kcal/mol). Figure 12d illustrates NT4 – C4 complex with a binding affinity score of -7.1 (kcal/mol) and binding pockets.

Molecular interaction complexes NT3—C5, NGF—C2, NGF—C5 & p75NTR—C1 were depicted in Fig. 13. Complex NT3—C5 interacts with a binding affinity of − 7 (kcal/mol) and active sites TYR 53, VAL 86, TYR 51, LYS 49 (Fig. 13a). NGF—C2 complex results binding affinity of − 8.7 (kcal/mol) with active site HIS 353 (Fig. 13b). NGF—C5 complex form interaction by binding pockets (Fig. 13c) with a binding score of − 7 (kcal/mol). Figure 13(d) describes the interaction of p75NTR—C1with active sites and binding affinity − 7.3 (kcal/mol).

In Fig. 14, Fig. 14a represent p75NTR—C2 complex with binding pockets ASP 15, VAL 133, LYS 58 and binding affinity − 7.6 (kcal/mol) whereas Fig. 14b depicts p75NTR—C4 complex with binding pockets and binding affinity − 7.8 (kcal/mol). p75NTR—C5 complex shows a binding affinity of − 8.5 (kcal/mol) with binding pockets ASP 72, THR 140, HIS 74, LYS 73, VAL 141, ASP 71, PRO 138 in Fig. 14c. p75NTR—C7 complex was represented in Fig. 14d with active sites and binding affinity − 8 (kcal/mol). From these twelve interactions, NT4-C3 complex exhibited the highest binding affinity score of − 10.4 (kcal/mol) followed by NGF-C2 (Fig. 12) complex

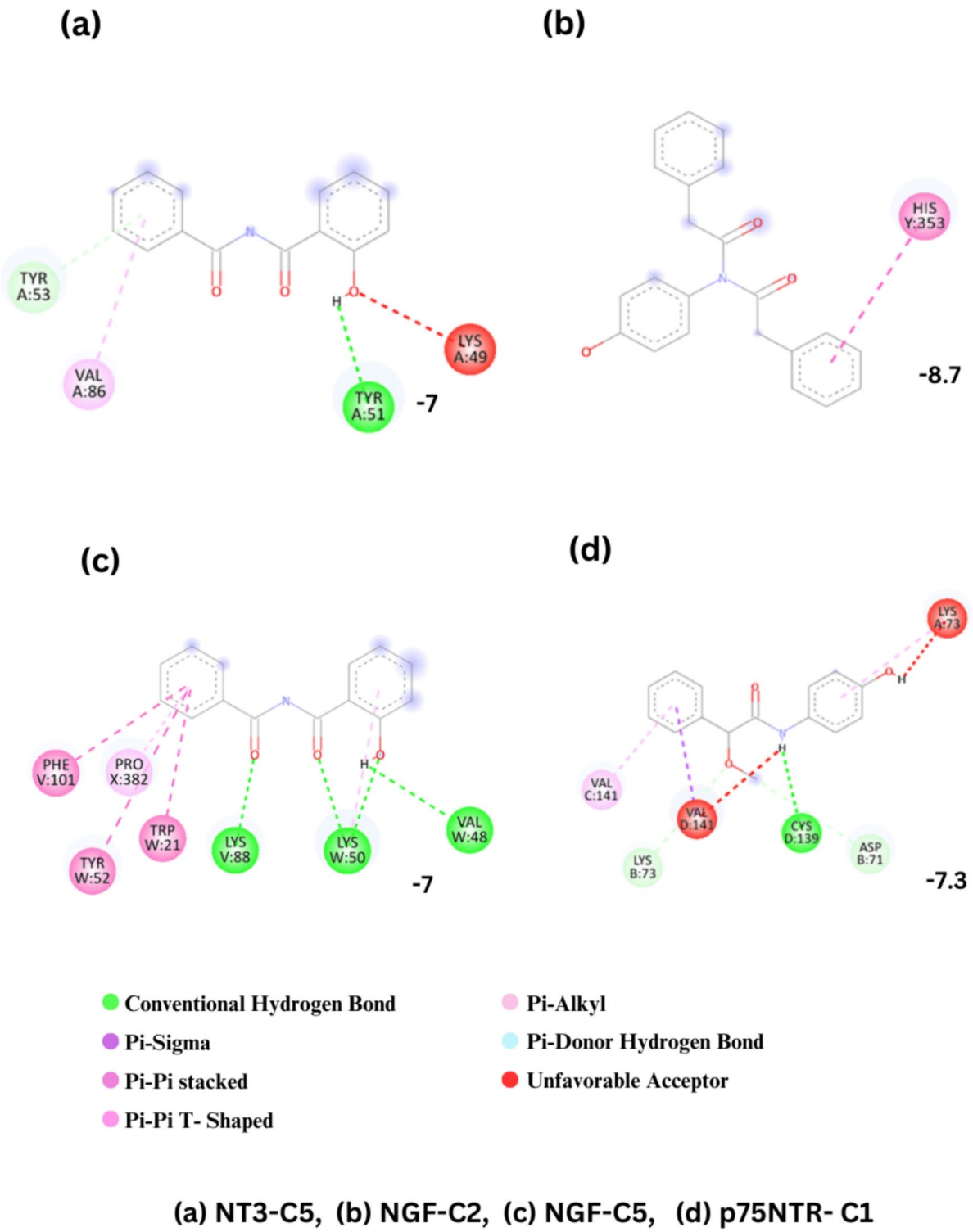

Fig. 13 Visualized molecular docking interacting complexes; **a** NT3-C5, **b** NGF-C2, **c** NGF-C5 & **d** p75NTR-C1

with a score of − 8.7 (kcal/mol) (Fig. 13), p75NTR-C5 complex with − 8.5 (kcal/mol) (Fig. 14) and p75NTR-C7 (Fig. 14) complex with -8 (kcal/mol) as binding affinity value (Ragunathan et al. 2022).

Molecular dynamic simulations

The interaction between the atoms and the molecules among temporal scales were measured using Molecular Dynamic

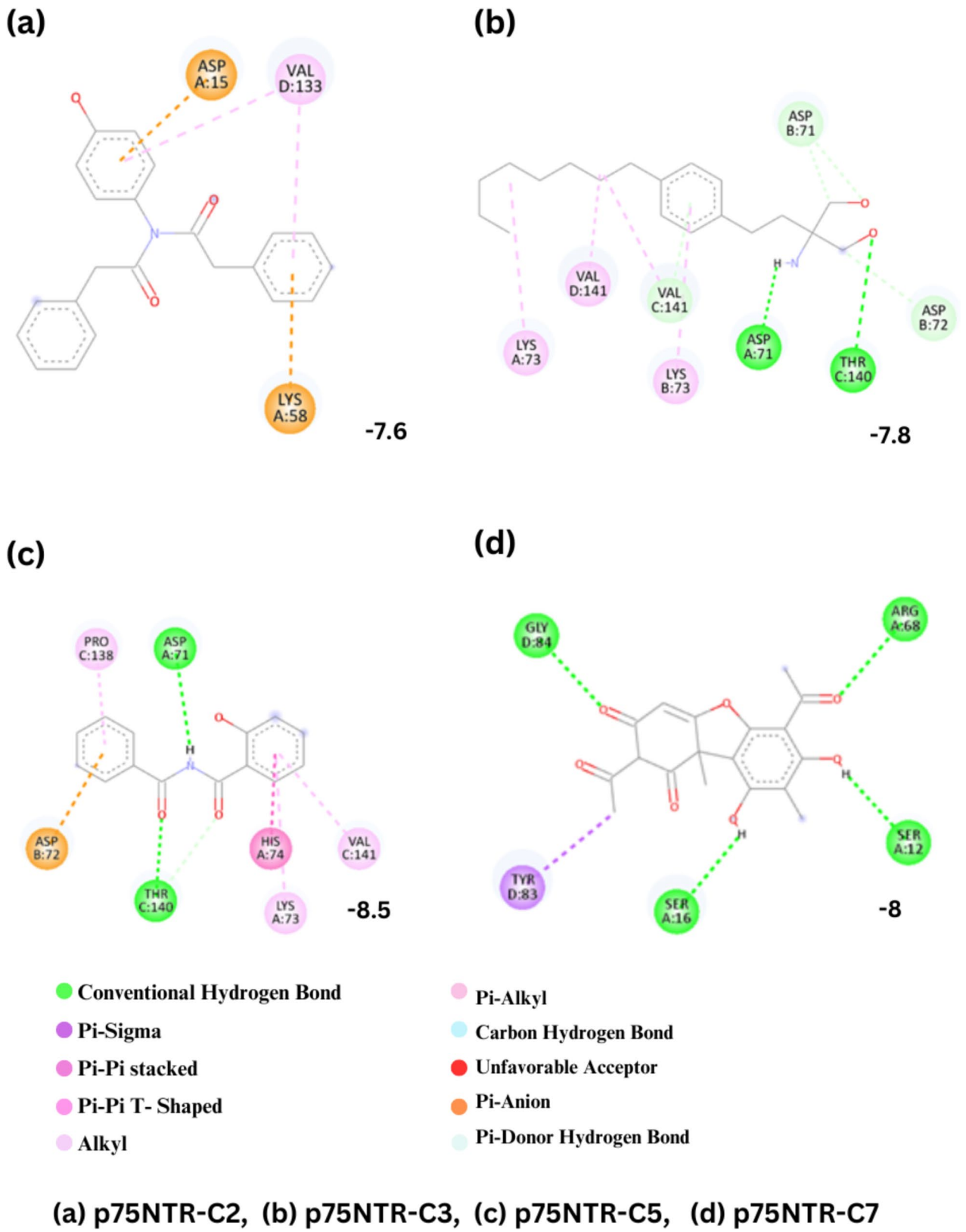

Fig. 14 Visualized molecular docking interacting complexes; **a** p75NTR-C2, **b** p75NTR-C3, **c** p75NTR-C5 & **d** p75NTR-C7

Table 11 The MD simulation parameters of the selected targets

PDB ID	Parameters	Energy (KJ/mol)	Err. Est	RMSD	Tot-drift (KJ/mol)
1B8K	Potential	−1.10577E+06	23,000	67,190.8	−146,887
	Temperature (K)	299.72	0.18	3.05599	1.06414
	Pressure (bar)	−3.33764	3.1	107.115	2.59275
	Density (SI)	1005.41	0.13	2.46874	0.832885
1BND	Potential	−1.10439E+06	19,000	49,939.8	−125,353
	Temperature (K)	299.773	0.19	3.06749	1.44257
	Pressure (bar)	−333.764	3.3	120.369	14.9891
	Density (SI)	1016.14	0.27	2.59602	1.85149
1B98	Potential	−1.12835E+06	25,000	86,274.5	−488,686
	Temperature (K)	299.954	0.26	3.07265	1.43568
	Pressure (bar)	−256.489	4.5	134.598	18.3654
	Density (SI)	995.26	0.54	2.5896	1.57486
1WWW	Potential	−3.76519E+06	62,000	423,118	−395,189
	Temperature (K)	299.824	0.15	3.05492	1.26548
	Pressure (bar)	−252.68	140	4992.33	875.432
	Density (SI)	1010.82	0.13	2.46874	0.832885

Table 12 Protein regulation by query protein BDNF, NT4, p75NTR, NGF and NT3 in down regulated protein

GENE	P val	FDR	GENE	P val	FDR
TET1	0.00129	0.22663	IRF2	0.00286	0.11834
GMEB1	0.00215	0.22663	MZF1	0.00454	0.16498
ZNF281	0.00244	0.22663	ZNF263	0.00478	0.16498
NFKB1	0.00274	0.22663	TFAP2A	0.00773	0.24255
SP1	0.00149	0.06225	EP300	0.00867	0.24255
MZF1	0.0015	0.06225	EGR4	0.00879	0.24255
DNMT1	0.00188	0.07066	RREB1	0.00102	0.05266
RREB1	0.00296	0.10201	E2F6	0.00137	0.05861
ZNF263	0.00408	0.13008	DNMT1	0.00142	0.05861
INSM1	0.00502	0.14852	ZNF202	0.00175	0.06575
ZNF281	0.00576	0.15897	GCM1	0.00311	0.10719
KLF5	0.00674	0.1745	EGR1	0.00387	0.12314
PAX4	0.01001	0.24373	TFAP2C	0.00445	0.13156
ZNF202	0.00108	0.05581	SP2	0.00586	0.16178
TFAP4	0.00268	0.11834	MZF1	0.00883	0.21746
KLF7	0.00893	0.21746	MZF1	0.01232	0.24285
ZNF281	0.01014	0.23318	EGR2	0.01282	0.24285
CGBP	0.01151	0.24285	MYB	0.01291	0.24285
EGR3	0.01362	0.24524			

(MD) Simulations performed using GROMACS for the target protein within the Google Colab platform where the protein structures were simulated at 100 ns. The study was conducted at a room temperature of 300 K and showed minimal fluctuations for four proteins. Following an initial visual examination of the trajectory, a more comprehensive assessment was carried out to ensure the simulation's quality. This evaluation of stability involved verifying the convergence of thermodynamic factors like temperature, pressure, potential, and density, and these energy minimization plots of Neurotrophins were given in Figs. 1, 2, 3, and 4. Overall, the stability analysis aimed to determine if equilibrium had been achieved. Structural convergence was assessed using the Root Mean Square Deviation (RMSD) between the initial and mean structures of the target protein. The stability study parameters of four target proteins were given in Table 11.

Discussion

The pathogenesis of ameloblastoma is mainly due to the proliferation of two types of cells, ie. anti-apoptotic activity due to peripheral ameloblast and the other by proapoptotic activity exhibited by central stellate reticulum cells. MAPK and BRAF proteins are the only recent advancement related to this odontogenic tumor in recent times and the metabolic pathway studies concluded that the Neurotrophin signaling pathway can act as new treatment methods (Yoithapprabhunath et al. 2020; Jisha et al. 2020; Renugadevi et al. 2020; Prabhunath et al. 2021). The key proteins involved in this Neurotrophin signaling pathway [NGF (Nerve Growth Factors), BDNF (Brain-Derived Neurotrophin Factor), P75 Neurotrophin Receptor (p75NTR), Neurotrophin 3 (NT3) and Neurotrophin 4 (NT4) were taken for gene prediction and the interacting proteins are identified using STRING analysis; based on the WNL values the leader genes were identified as these genes might have a major role in the

pathophysiology of Ameloblastoma. Selection of top WNL values as leader genes were assessed based on the previous research elaborating STRING analysis (Szklarczyk et al. 2014).

From K mean clustering and Kruskal Walli's test it is identified that proteins BDNF, NT4, p75NTR and NGF are significant (having similarities across clusters or unsupervised algorithm) along the cluster and it is evenly distributed among the various clusters, indicating that each cluster contributes equally to the control and operation of the Neurotrophin signaling pathway even if it may comprise distinct cell types or states. The results of NT3 Protein Analysis, the leader genes are significantly present in Clusters 1 and 2, but not in Cluster 3, which has a lower level and is determined to be non-significant reveling that important proteins, or leader genes, are distributed differently among the clusters. Comparing Cluster 3 to Clusters 1 and 2, the decreased presence of significant genes in Cluster 3 would suggest that it plays a less role in the NT3-related metabolic pathways.

Numerous proteins were found to be both up- and down-regulated in the Neurotrophin signalling pathway according to the results of ontology analysis. Among these proteins, a few are primarily engaged in particular functions that have been documented in earlier research, as detailed in Tables 8, 12. Topology analysis reveals that the proteins NT4, NGF, and BDNF are highly interconnected within the Neurotrophin signaling pathway, evidenced by their substantial clustering coefficient values. These proteins are central to the network, with BDNF connecting to an average of 14.80 neighbors, NT4 to 13.12, and NGF to 10.2. Unlike p75NTR and NT3, which do not form multiple edges, BDNF, NT4, and NGF create numerous connections, highlighting their role as potential key targets in the pathway. The order of network density for these proteins confirms their importance, with NT4 ranking the highest, followed by BDNF and NGF, indicating their critical roles in maintaining the integrity and functionality of the Neurotrophin signaling network.

The ability of ligands Methyl-ɣ-oresellinate, N-(4-Hydroxy-phenyl)-2-phenyl-N-phenylacetyl-acetamide, Atranorin, and Oresellinate to form interaction with target protein was observed during further interaction of the ligands with selected proteins using molecular docking tools. Drug compounds with binding affinity values below -8 (kcal/mol) were selected as effective ligands in previous studies. In terms of binding affinity, NT4–C3 demonstrated the highest value at -10.4 (kcal/mol), whereas NGF–C2 complex displayed the second-highest value at – 8.7 (kcal/mol). Both proteins displayed significant clustering coefficient values in topological analysis. Based on more research, it is feasible that NGF and NT4 could be employed as therapy drugs because of their high levels of interlinkage with pathway proteins that make them appropriate as targets. Additionally, ligands C2 and C3 may operate as potential ligands for these target proteins and might be used as a possible drug of choice for the treatment based on further studies.

Conclusion

The study confirm that the Neurotrophin signaling pathway makes a notable effect on cell proliferation, differentiation, and cell survival through NF-kB, PI3K/AKT, MAPK/ERK, and PLCγ/PKC signalling cascade associated with Ameloblastoma which could be a possible reason for the molecular pathogenesis. The current study may paw a way for therapeutic intervention by targeting these proteins.

Supplementary Information The online version contains supplementary material available at https://doi.org/10.1007/s40203-024-00223-2.

Author contributions Mr. MV & Ms. DR carried out experiment, Dr. SS & Dr. SZA hypothesized, drafted and coordinated all the experiments and represented to be a correspondence of the manuscript. Dr. YTR & Dr. SK involved and helped during the assessment of genes related to ameloblastoma, Dr. PP supervised in-silico analysis. All authors read and approved the final manuscript.

Data availability All data are included in the Manuscript and in supplementary file.

Declarations

Conflict of interest The authors declare no competing interests.

References

Abdelhalim DA, Elgamal BM, ElKafoury MR, Hassan NM, Hussein MM, Elhefnawi MM, Elfiky AM, Nabil M (2018) MicroRNA-150 down regulation in acute myeloid leukaemia patients and its prognostic implication. J Med Sci. 6(11):1993–2000. https://doi.org/10.3889/oamjms.2018.420

Arunachalam T, Khader SZA, Ahmed SSZ, Vetrivel M, Tajudeen SAS, Sheriff AKI, Prabhu P, Jayachandran PR, Sabu Dastageer M (2019) Radical scavenging and antiproliferative effect of novel phenolic derivatives isolated from *Nerium indicum* against human breast cancer cell line (MCF-7)—an in silico and in vitro approach. Env Sci Poll Res 27:9038–9057. https://doi.org/10.1007/s11356-019-07252-x

Assenov Y (2008) Computing topological parameters of biological networks. Bioinformatics 24(2):282–284. https://doi.org/10.1093/bioinformatics/btm554

Azmi MB, Khan F, Asif U, Khurshid B, Wadood A, Qureshi SA, Ahmed SDH, Mudassir HA, Sheikh SI, Feroz N (2023) In Silico characterization of withania coagulans bioactive compounds as potential inhibitors of hydroxymethylglutaryl (HMG-CoA) reductase of mus musculus. ACS Omega 8(5):5057–5071. https://doi.org/10.1021/acsomega.2c07893

Capriotti R, Calabrese R, Casadio R (2006) Predicting the insurgence of human genetic diseases associated to single point protein mutations with support vector machines and evolutionary information. Bioinformatics 22(22):2729–2734. https://doi.org/10.1093/bioinformatics/btl423

Crow M, Lim N, Ballouz S, Pavlidis P, Gillis J (2019) Predictability of human differential gene expression. Proc Natl Acad Sci 116(13):6491–6500. https://doi.org/10.1073/pnas.1802973116

Ding Z, Kihara D (2019) Computational identification of protein-protein interactions in model plant proteomes. Sci Rep. 9(1):8740. https://doi.org/10.1038/s41598-019-45072-8

Forli S, Huey R, Pique ME, Sanner MF, Goodsell DS, Olson AJ (2016) Computational protein-ligand docking and virtual drug screening with the AutoDock suite. Nat Protoc 11(5):905–919. https://doi.org/10.1038/nprot.2016.051

Jisha GB, Ilayaraja V, Yoithapprabhunath TR, Ganapathy N, Dineshshankar J, Nirmal RM (2020) Immunohistochemical detection of Tyrosine Kinase receptor (TrK) in follicular and plexiform ameloblastoma—a noval study. J Oral Maxillofac Pathol. 24(1):125–130. https://doi.org/10.4103/2Fjomfp.JOMFP_220_19

Marin C, Dave M, Hunter KD (2021) Malignant odontogenic tumours, front oral health: a systematic review of cases reported in literature. Front. Oral. Health. 2:775707. https://doi.org/10.3389/froh.2021.775707

Masthan KMK, Anitha N, Krupaa J, Manikkam S (2015) Ameloblastoma. J Pharm Bio Allied Sci. 7(5):167. https://doi.org/10.4103/0975-7406.155891

Orlando B, Bragazzi N, Nicolini C (2013) Bioinformatics and systems biology analysis of genes network involved in OLP (Oral Lichen Planus) pathogenesis. Arch Oral Biol 58(6):664–673. https://doi.org/10.1016/j.archoralbio.2012.12.002

Prabhunath TRY, Nirmal R, Veeravarmal V, Dineshshankar J, Amsaveni R (2021) Immunohistochemical analysis of nuclear factor-kappa B (NF-κB) between follicular and plexiform ameloblastomas: a pilot study. J Oral Maxillofac Pathol 24:466–471. https://doi.org/10.4103/jump.JOMFP_150_20

Ragunathan V, Tiwari P (2022) Molecular docking, validation, dynamics simulations and pharmacokinetic prediction of natural compounds against the SARS-CoV-2 main-protease. J Biomol Struct Dyn 40(2):585–611. https://doi.org/10.1080/07391102.2020.1815584

Rao VS, Srinivas K, Sujini GN, Kumar GN (2014) Protein-protein interaction detection: methods and analysis. Int J Proteomics 2014:147648. https://doi.org/10.1155/2014/147648

Renugadevi S, Ganapathy N, Dineshshankar J, Yamunadevi A, Nirmal M, Ragunathan T, Prabhunath Y (2020) Immunohistochemical detection of Nerve Growth Factor (NGF) in follicular and plexiform ameloblastoma: a novel study. J Pharm Bioall Sci 12:569–575. https://doi.org/10.4103/jpbs

Santos EM, Santos HO, Dos SantosDias I, Santos SH, de BatistaPaula AM, Feltenberger JD, SenaGuimarães AL, Farias LC (2016) Bioinformatics analysis reveals genes involved in the pathogenesis of ameloblastoma and keratocystic odontogenic. Tumor Int J Mol Cell Med. 5(4):199–219. https://doi.org/10.22088/ACADPUB

Syed Zameer Ahmed K, Sidhra S, Thangakumar A (2021) Isolation of novel compounds from *Parmotrema reticulatum* for treating arthritis. Indian Patent 363466, 29 Mar 2021.

Syed Zameer Ahmed K, Sidhra S, Thangakumar A, Syed Tajudeen (2023a) Novel phenolic compounds from *Nerium indicum* with anti - breast cancer activity. Indian Patent 420602, 06 Feb 2023.

Syed Zameer Ahmed K, Sidhra S, Thangakumar A (2023b) Therapeutic effect of *Parmotrema tinctorum* against complete freund's adjuvant-induced arthritis in rats and identification of novel isophthalic ester derivative. Indian Patent 428986, 13 Apr 2023.

Szklarczyk D, Franceschini A, Wyder S, Forslund K, Heller D, Huerta-Cepas J, Simonovic M, Roth A, Santos A, Tsafou KP, Kuhn M, Bork P, Jensen LJ, von Mering C (2014) STRING v10: protein-protein interaction networks, integrated over the tree of life. Nucleic Acids Res 43:D447–D452. https://doi.org/10.1093/nar/gku1003

Thomaz A, Jaeger M, Brunetto AL, Brunetto AT, Gregianin L, de Farias CB, Ramaswamy V, Nor C, Taylor MD, Roesler R (2020) Neurotrophin signaling in medulloblastoma. Cancers Basel 12(9):2542. https://doi.org/10.3390/cancers12092542

Trott O, Olson AJ (2010) AutoDock Vina: improving the speed and accuracy of docking with a new scoring function, efficient optimization and multithreading. J Comput Chem 31(2):455–461. https://doi.org/10.1002/jcc.21334

Walden JP, Hoggarth JA, Ebert CE, Fedick SL, Biggie M, Meyer B, Shaw-Müller K, Qiu Y, Ran W, Ellis OP, Watkins TB, Davis JB, Guerra RA, Helmke C, Awe JJ (2023) Classic Maya settlement systems reveal differential land use patterns in the upper Belize River Valley. Land 12(2):483. https://doi.org/10.3390/land12020483

Yoithapprabhunath TR, Rachel Sarah Vinodhini K, Mohanapriya S, Raj JBS, Kalaiselvi V, Nirmal RM (2020) Neurotrophins (NTs) and Neurotrophin Receptors (NTRs) as emerging therapeutic paradigm in head and neck tumors—a mini review. J Indian Acad Oral Med Radiol. 32(3):278–283. https://doi.org/10.4103/jiaomr.jiaomr_125_20

Publisher's Note Springer Nature remains neutral with regard to jurisdictional claims in published maps and institutional affiliations.

Springer Nature or its licensor (e.g. a society or other partner) holds exclusive rights to this article under a publishing agreement with the author(s) or other rightsholder(s); author self-archiving of the accepted manuscript version of this article is solely governed by the terms of such publishing agreement and applicable law.